Defect formation in graphene nanosheets by acid treatment: an x-ray absorption spectroscopy and density functional theory study

2008 J. Phys. D: Appl. Phys. 41 062001

(http://iopscience.iop.org/0022-3727/41/6/062001)

IOP PUBLISHING
IOP FTC
JOURNAL OF PHYSICS D: APPLIED PHYSICS
J. Phys. D: Appl. Phys. **41** (2008) 062001 (4pp)
doi:10.1088/0022-3727/41/6/062001

FAST TRACK COMMUNICATION

Defect formation in graphene nanosheets by acid treatment: an x-ray absorption spectroscopy and density functional theory study

V A Coleman[1], R Knut[1], O Karis[1], H Grennberg[2], U Jansson[3], R Quinlan[4,5], B C Holloway[5], B Sanyal[1] and O Eriksson[1]

[1] Department of Physics, Box 530, Ångström Laboratory, Uppsala University, 751 21 Uppsala, Sweden
[2] Department of Biochemistry and Organic Chemistry, Box 576, Uppsala University, 751 23 Uppsala, Sweden
[3] Department of Materials Chemistry, Box 538, Ångström Laboratory, Uppsala University, 751 21 Uppsala, Sweden
[4] Department of Applied Science, College of William and Mary, 325 McGlothin Street Hall, Williamsburg, VA 23187, USA
[5] Luna Innovations, NanoWorks Division, 521 Bridge Street, Danville, VA 24541, USA

E-mail: Ulf.Jansson@mkem.uu.se

Received 27 January 2008
Published 21 February 2008
Online at stacks.iop.org/JPhysD/41/062001

Abstract
In-plane defects have been introduced into graphene nanosheets by treatment with hydrochloric acid. Acid treatment induces bond cleavage in the C–C network via electrophilic attack. These resultant vacancy sites will then undergo further reactions with the surrounding ambient to produce C–O and C–H bonds. A σ^* resonance at 287 eV in the carbon K-edge x-ray absorption spectra is observed with acid treatment and is assigned to C–O states. Theoretical modelling of a di-vacancy in a graphene bilayer reproduces all essential features of this resonance and in addition predicts a metallic conductivity of states around this vacancy. The possibility of engineering the properties of graphene via the routes explored here is an important step towards establishing strategies for building devices based on this material.

(Some figures in this article are in colour only in the electronic version)

Graphene is an emerging material from the carbon family which possesses a host of exciting opportunities for novel, nanostructured device applications [1]. To date, the most exploitable feature of graphene aside from its low dimensionality has been the edges of nanosheets and ribbons where interesting electronic properties and sites for functionalization develop [2, 3]. In particular, metallic states have been identified for certain edge structures [3]. Such sites are, however, inherently limited by their structure, edge to volume ratio and method of fabrication. By envisaging defect creation over a whole graphene sheet, these issues can be overcome, opening up a host of new opportunities, including functionalized membranes and catalytic supports.

Acid treatment is known to create defects in carbon nanotubes [4–6] and should also form defects in graphene, representing a cheap, controllable, simple and scaleable method for defect formation. Use of a non-oxidizing acid such as HCl where only hydronium ions will take part in

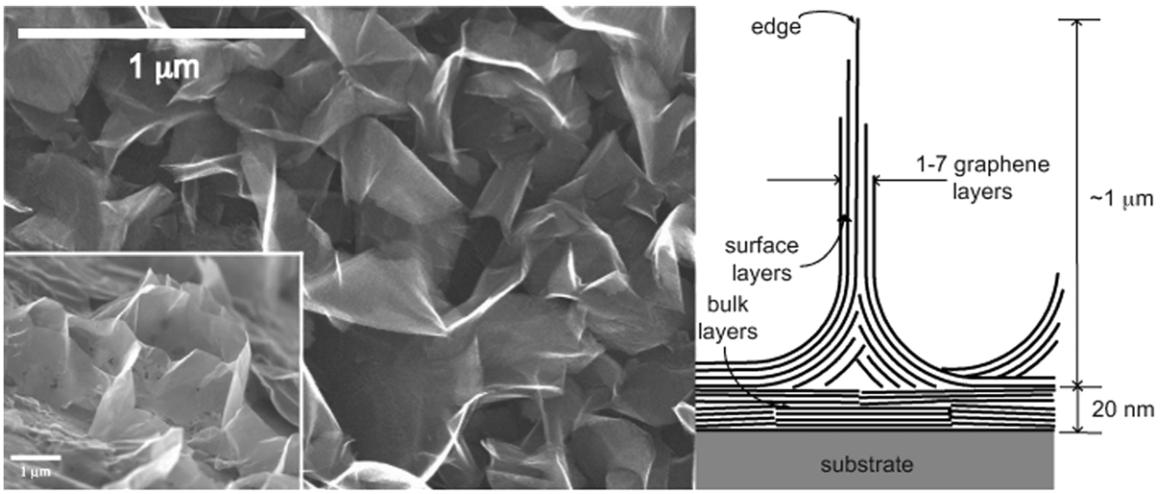

Figure 1. (Left) A plan-view SEM image of an as-grown sample. The inset shows a side-on SEM image of the acid treated sample. (Right) Schematic diagram illustrating the structure of the samples.

the initial defect formation process [7] opens possibilities for varying the electronic properties around the defect site with functional group addition. This would also enable further functionalization via the initially added groups in the graphene layers.

A significant amount of literature is currently available on modelling vacancy defects in graphene [8, 9], where several interesting properties have been speculated to result. Specifically, vacancy defects are predicted to change the semimetallic character to metallic [8], whilst the energetics of the dissociation of several molecular species (e.g. H_2O) have also been shown to be dramatically influenced [9].

Currently however, there are no solid experimental studies to support these theoretical studies. X-ray absorption spectroscopy (XAS) studies of pure graphene have been conducted [10, 11]; however, there are no significant studies of defects in the graphene system. More extensive studies on graphite and carbon nanotubes exist [12, 13], where the presence of defect states is noted and assigned to either C–H, C=O or C–O. In this study we combine synthesis methods, angular dependent XAS measurements around the carbon K-edge and theoretical modelling of a graphene bilayer system to investigate defect creation in graphene. This is the first step towards functionalization of graphene and graphene-like materials in a novel fashion and paves the way for new and improved properties of this class of materials.

In the experimental studies, we have used a well-defined and controlled carbon nanosheet (CNS) system consisting of standing structures made up of 1–7 graphene layers perpendicular to the substrate surface (see figure 1) [14]. The sheets are $\sim$1 μm high and are formed on top of a $\sim$20 nm thick graphite-like film. The CNSs were grown by radio frequency plasma enhanced chemical vapour deposition (RF PECVD), on tungsten foils (0.1 mm thick). Precise synthesis details as well as thorough characterization of the as-grown nanosheets has been previously reported and will not be reproduced here [14].

Following deposition, one sample, henceforth referred to as the 'acid treated' sample, was treated with concentrated HCl (35%) at 90 °C for 4 h. After this, HCl residue was removed by washing with deionized water and the sample was dried in air at 150 °C for 3 min. A 'control' sample was prepared in an identical manner, using deionized water instead of HCl. Prior to treatments, both samples showed hydrophobic behaviour. Acid treatment results in improved wettability. This suggests that HCl treatment results in the addition of polar OH groups to the CNSs. SEM characterization of both samples was then conducted to verify the integrity of CNSs.

XAS measurements were conducted at beamline D1011 at MAX II, MAX-Lab, Sweden. Prior to all measurements, the samples were heated *in situ* to 170 °C overnight, to remove surface adsorbates [15]. XAS measurements around the C K-edge were recorded in total electron yield mode. The angle of the sample with respect to the incident beam was varied such that the reported angle is the angle between the substrate normal and the incident beam. Following measurements, the XAS spectra were corrected by the incident photon flux, monitored on a clean Au grid, and pre-edge normalized. A linear background was then subtracted, followed by post-edge normalization (at 320 eV).

The left panel of figure 1 shows an SEM image of the as-deposited sample. In this image, the freestanding CNSs can be clearly seen emerging from the graphite-coated substrate. The inset shows a side-on (arbitrary angle) SEM image taken from the sample following acid treatment which does not result in any obvious changes to the samples.

Figure 2 shows the XAS spectra recorded from the control (solid lines) and acid treated (dotted lines) samples at three different angles; 0° (normal incidence), 45° and 80° (grazing incidence). In all spectra, three main features are obvious. The first, labelled A, arises from π^* C–C resonances. The second, B1 and B2, are associated with defects in the graphene system. In other low-dimensional carbon systems, these features have been attributed to π^* C=O, σ^* C–O and σ^* C–H resonances [12, 13]. The third set of features, C1 and C2, are σ^* C–C resonances.

It is evident that features A, C1 and C2 do not show the angular dependence expected for π^* and σ^* resonances in a system of only freestanding graphene. For such a case,

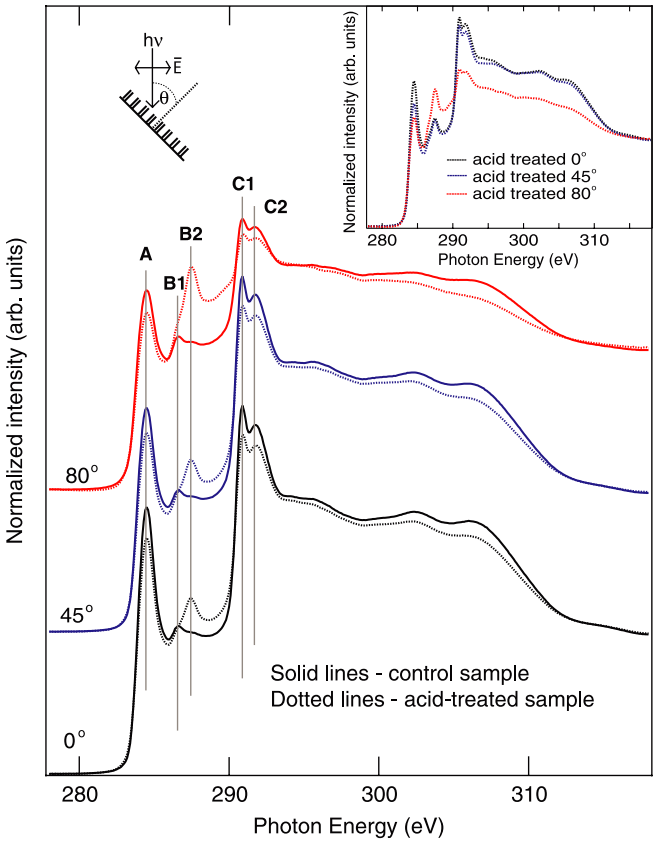

Figure 2. Comparative carbon K-edge XAS spectra from the 'control' and 'acid treated' samples, at three different angles of beam incidence. The labels A, B1, B2, C1 and C2 indicate the main features of interest. The spectra have been pre- and post-edge normalized and the energy resolution is 100 meV. The inset provides a direct angular comparison for the acid treated sample. The measurement geometry is shown in the top left corner.

the π^* resonance (feature A) would have maximum intensity at grazing incidence and minimum intensity at normal incidence, whilst the σ^* resonance (features C1 and C2) would display the opposite behaviour. In this system, we observe a strong intensity contribution from both resonances at all angles. This is because the system consists of a layer of graphite in the substrate plane in addition to the freestanding CNSs, as shown in figure 1. The signal from the graphite in the substrate plane will display the opposite angular dependence to that of the freestanding sheets and a sum of these two contributions is measured at each angle.

Both samples exhibit B1 and B2 features but with different intensities. The features are small in the control sample, indicating that the number of defects is significantly lower than in the acid treated sample. The latter exhibits a dramatically increased B2 feature, whilst feature B1 appears to remain constant. Feature B2 is due to defects introduced by the acid treatment and with different characters than the defects responsible for the B1 peak. We attribute the B2 feature to C–O bonds, formed by bond cleavage in the C–C network with addition of OH groups. This hypothesis is supported by (1) the improved wettability of the CNSs, (2) the decrease in the intensity of the A and C resonances corresponding to a relative decrease in C–C π^* and σ^* transitions and (3) x-ray photo electron spectroscopy (XPS) studies (not shown), which indicate that the acid treated sample has a 30% higher O : C ratio compared with the control sample and 100% higher O : C ratio compared with an as-deposited sample, which contained 2–3% O. Finally, the absence of Cl in XPS spectra excludes the possibility of C–Cl bonds as the origin of the B2 feature.

It is evident that the B2 resonance is most pronounced at grazing incidence (inset, figure 2). It can be assumed that the free standing graphene sheets exposed to acid will be the most susceptible to electrophilic attack by the hydronium ion [7]. Consequently, most bond cleavages will occur on the surface layers of the free standing CNSs, leaving the graphite parallel to the substrate mostly unaffected. Our results hence imply that the B2 resonance possesses σ^* character, i.e. involving σ bonds within the CNS plane.

The left panel of figure 3 depicts a model of a di-vacancy, one of the defects that acid treatment is likely to produce in the graphene planes. The atoms around the vacancy will not maintain highly reactive unsaturated dangling bonds; groups such as OH will bind to these sites in order to satisfy the valency requirement of the C atoms. Thus oxygen atoms bind to the defects via sp^2 orbitals supporting the observation of the σ^* resonance at B2.

Theoretical calculations were performed using density functional theory as implemented in the Vienna Ab-initio Simulation Package (VASP) [16]. The projector augmented wave basis was used with a plane wave cut-off energy of 400 eV. We used generalized gradient approximation for the treatment of exchange-correlation functional. A di-vacancy was created by taking away two neighbouring carbon atoms from one layer of the bilayer graphene used in the calculations with a unit cell containing 100 atoms, yielding a structure much the same as that shown in the left panel of figure 3. Equilibrium geometry of the bilayer graphene was determined by relaxing the atomic positions until the Hellmann–Feynman forces converged within an accuracy of 0.02 eV $Å^{-1}$. Calculations of a pure graphene layer were performed for comparison.

The calculated density of states (DOS) are shown on the right of figure 3. The top panel shows a comparison between a pure graphene layer and a bilayer graphene containing a di-vacancy, and the middle and lower panels show the DOS projected onto C atoms close to and far away from the di-vacancy, respectivley. The carbon atom situated close to the vacancy has a completely different electronic structure compared with the ones far from the defect site. Specifically, a metallic component develops with electron states of p_z character at the Fermi level, E_F, for atoms around the defect. In addition a peak 3–4 eV above E_F appears for atoms close to the defect. This feature is consistent with the experimental finding of peak B2 located between the π^* and σ^* states. For a normal carbon atom (far from the defect), the p_x and p_y states coincide and form the in-plane σ bond, whereas the out-of-plane p_z orbital forms the π bond (figure 3). Due to decreased symmetry close to the defect site, the p_x and p_y orbitals are no longer degenerate (middle panel of figure 3). The vacancy induced state has in-plane σ character (see left panel of figure 3). Calculations incorporating species attached to dangling bonds around the defect, such as atomic H attached to defect sites, do not change the main features of figure 3 (data not shown).

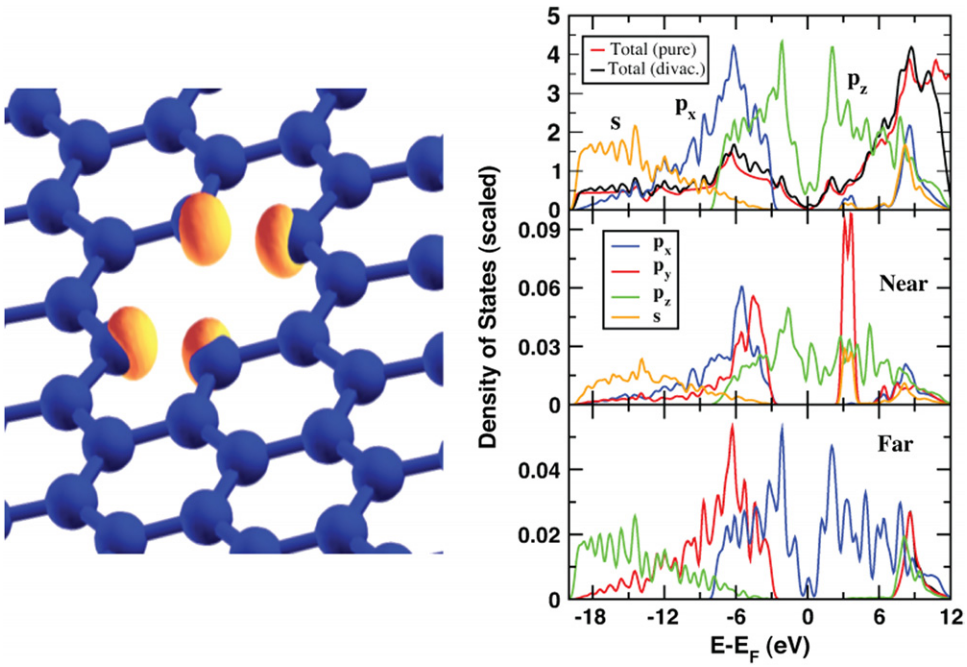

Figure 3. In the right panels, the calculated DOS: (top) total DOS for pure graphene layer and a bilayer graphene with a di-vacancy, (middle) m_l-projected DOS for a carbon atom close to the di vacancy and (bottom) same but for a carbon atom far from the vacancy site. On the left part of the figure the charge density of the electron states induced by the defect, in the energy region of 3–4 eV above the Fermi level, is shown.

The fact that theory reproduces the vacancy induced spectroscopic feature (peak B2) gives credence to the accuracy of the calculations. Hence, other features of the calculations, e.g. the metallic character of atoms around the defects, which are not being measured directly here, are likely to be reliable as well. For this reason we conclude that, when taking the experimental and theoretical results together, it is possible, via a very efficient acid treatment in HCl, to produce defects in CNSs that induces electronic properties distinctly different from those of pure graphene. Our results are also significant in that we have identified a way to achieve novel properties and novel functionality within a graphene layer. In particular, the metallic component of the electron states around the defects is important. This opens up possibilities to influence the transport properties of graphene, via the concentration of such defects. Such possibilities will be very important in establishing strategies for building graphene-based devices of this fascinating material.

Acknowledgments

The Swedish Research Council (VR) and the Swedish National Infrastructure for Computing (SNIC) are gratefully acknowledged. This material is based upon work supported by the United States Air Force under Contract No FA9550-06-C-0010. Any opinions, finding and conclusions or recommendations expressed in this material are those of the authors and do not necessarily reflect the views of the United States Air Force.

References

[1] Avouris P, Chen Z and Perebeinos V 2007 Carbon-based electronics *Nature Nanotechnol.* **2** 605
[2] Yan Q, Huang B, Yu J, Zheng F, Zang J, Wu J, Gu B-L, Liu F and Duan W 2007 *Nano Lett.* **7** 1469
[3] Son Y-W, Cohen M L and Louie S G 2006 *Nature* **444** 347
[4] Balasubramanian K and Burghard M 2005 *Small* **1** 180
[5] Itkis M I, Perea D E, Jung R, Nigoyi S and Haddon R C 2005 *J. Am. Chem. Soc.* **127** 3439
[6] Strano M S *et al* 2003 *J. Phys. Chem.* B **107** 6979
[7] Li J, Chajara K, Lindgren J and Grennberg H 2007 *J. Nanosci. Nanotechnol.* **7** 1525
[8] Peres N M R, Guinea F and Castro Neto A H 2006 *Phys. Rev.* B **73** 125411
[9] Allouche A and Fero Y 2006 *Carbon* **44** 3320
[10] Entani S, Ikeda S, Kiguchi M, Saiki K, Yoshikawa G, Nakai I, Kondoh H and Ohta T 2006 *Appl. Phys. Lett.* **88** 153126
[11] Cappelli E, Scilletta C, Orlando S, Flammini R, Iacobucci S and Ascarelli P 2005 *Thin Solid Films* **482** 305
[12] Kuznetsova A, Popova I, Yates J T Jr, Bronikowski M J, Huffman C B, Liu J, Smalley R E, Hwu H H and Chen J G 2001 *J. Am. Chem. Soc.* **123** 10699
[13] Banerjee S, Hemraj-Benny T, Balasubramanian M, Fischer D A, Misewich J A and Wong S S 2004 *Chem. Commun.* 772
[14] Wang J, Zhu M, Outlaw R A, Zhao X, Manos D M and Holloway B C 2004 Synthesis of carbon nanosheets by inductively coupled radio/frequency plasma enhanced chemical vapor deposition *Carbon* **42** 2867
[15] Zhao X, Outlaw R A, Wang J J, Zhu M Y, Smith G D and Holloway B C 2006 *J. Phys. Chem.* **124** 194704
[16] Kresse G and Furthmüller J 1996 *Phys. Rev.* B **54** 11169 and references therein.